

Synthesis, characterization, and multielectron redox property of pyridine-coordinated tetra-Ru-oxo core sandwich-type silicotungstate, $[(\gamma\text{-SiW}_{10}\text{O}_{36})_2\{\text{Ru(IV)(pyridine)}\}_4\text{O}_4(\text{OH})_2]^{10-}$

Kodai Kokumai,^[a] Sugiarto,^[a] and Masahiro Sadakane*^[a]

Abstract: A pyridine-coordinated tetra-Ru-oxo core sandwich-type silicotungstate, $[(\gamma\text{-SiW}_{10}\text{O}_{36})_2\{\text{Ru(IV)(pyridine)}\}_4\text{O}_4(\text{OH})_2]^{10-}$, in which four Ru atoms are coordinated by pyridine molecules, was prepared and characterized by single-crystal X-ray structure analysis, ^1H nuclear magnetic resonance spectroscopy (^1H NMR), high-resolution electrospray ionization mass spectrometry (HR-ESI-MS), infrared (IR) spectroscopy, and elemental analysis. Cyclic voltammetry and ultraviolet–visible (UV-Vis) electro spectroscopy indicated that the molecule showed multielectron redox processes over a wide pH range (1–12).

Introduction

Polyoxotungstates are anionic tungsten-based oxide molecules that can incorporate other elements into the molecule.^[1] Transition metal-containing polyoxotungstates are more robust than metal organic complexes under oxidative conditions. Therefore, many transition metal-containing polyoxotungstates have been prepared and utilized as oxidation catalysts^[2, 3]. Among them, $[(\gamma\text{-SiW}_{10}\text{O}_{36})_2\{\text{Ru(IV)(H}_2\text{O)}\}_4\text{O}_4(\text{OH})_2]^{10-}$ (Figure 1 (a) and (b)), in which a tetra-Ru-oxo core ($\{\text{Ru(IV)(H}_2\text{O)}\}_4\text{O}_4\text{OH}_2\}^{6+}$) is sandwiched between two γ -type di-lacunary Keggin-type silicotungstates ($[\gamma\text{-SiW}_{10}\text{O}_{36}]^{8-}$) reported by Mizuno et al.^[4], Bonchio et al.^[5] and Hill et al.^[6], has attracted considerable attention as a highly active catalyst for water oxidation^[7, 8] and alcohol oxidation^[9]. The interaction of anionic $[(\gamma\text{-SiW}_{10}\text{O}_{36})_2\{\text{Ru(IV)(H}_2\text{O)}\}_4\text{O}_4(\text{OH})_2]^{10-}$ with cationic organic species is one of the most utilized methods to modify the catalyst system^[10, 11]. However, there is only one report on the substitution of the water molecule coordinated to Ru, in which Cl^- is coordinated to Ru.^[4]

Mono-Ru-substituted polyoxotungstates react with organic molecules such as dimethylsulfoxide,^[12–14] carbon monoxide,^[15, 16] and pyridine^[17] causing changes in the redox potentials of Ru. Here, we show that water molecules coordinated to Ru(IV) in $[(\gamma\text{-SiW}_{10}\text{O}_{36})_2\{\text{Ru(IV)(H}_2\text{O)}\}_4\text{O}_4(\text{OH})_2]^{10-}$ are exchangeable with pyridine in aqueous solution, and a tetra-pyridine-coordinating derivative, $[(\gamma\text{-SiW}_{10}\text{O}_{36})_2\{\text{Ru(IV)(pyridine)}\}_4\text{O}_4(\text{OH})_2]^{10-}$, is

formed. Furthermore, the multielectron redox properties of this molecule are presented. This is the first example of an organic ligand in the tetra-Ru-oxo core complex.

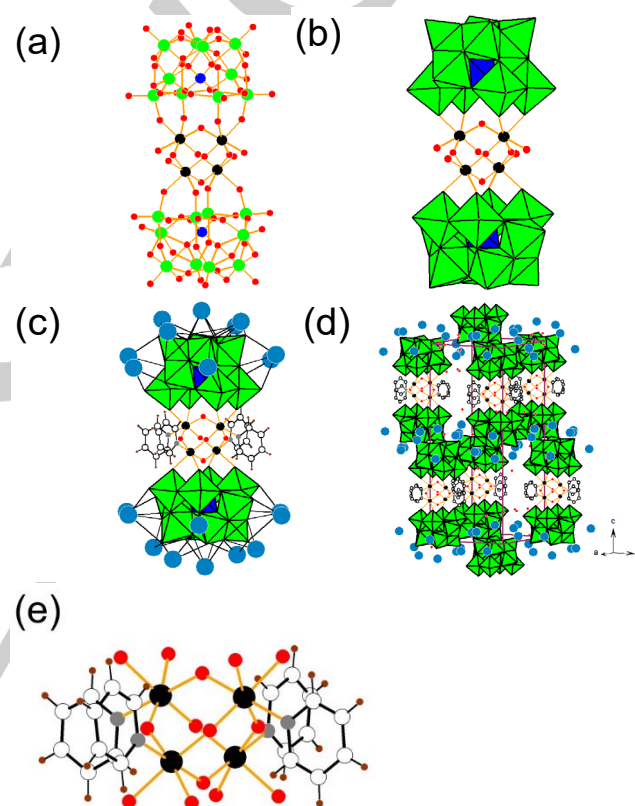


Figure 1. (a) Ball-and-stick representation and (b) polyhedral representation of $[(\gamma\text{-SiW}_{10}\text{O}_{36})_2\{\text{Ru(IV)(H}_2\text{O)}\}_4\text{O}_4(\text{OH})_2]^{10-}$. (c) Polyhedral representation of $[(\gamma\text{-SiW}_{10}\text{O}_{36})_2\{\text{Ru(IV)(pyridine)}\}_4\text{O}_4(\text{OH})_2]^{10-}$ with cesium counter cations and (d) packing of $[(\gamma\text{-SiW}_{10}\text{O}_{36})_2\{\text{Ru(IV)(pyridine)}\}_4\text{O}_4(\text{OH})_2]^{10-}$. (e) Ball-and-stick representation of the $\{\text{Ru(IV)(pyridine)}\}_4\text{O}_4(\text{OH})_2$ core. Green, blue, black, red, gray, light blue, white, and brown balls represent W, Si, Ru, O, N, Cs, C, and H atoms, respectively.

Results and Discussion

Preparation and structural characterization of $\text{Cs}_9\text{K}[(\gamma\text{-SiW}_{10}\text{O}_{36})_2\{\text{Ru(IV)(pyridine)}\}_4\text{O}_4(\text{OH})_2]$. A cesium–potassium mixed salt of $[(\gamma\text{-SiW}_{10}\text{O}_{36})_2\{\text{Ru(IV)(H}_2\text{O)}\}_4\text{O}_4(\text{OH})_2]^{10-}$ and ~100 equiv. of pyridine were mixed in water, and the mixture was heated at 80 °C for 3 h. The cyclic voltammogram of the reaction

[a] Mr. K. Kokumai, Dr. Sugiarto, Prof. Dr. rer. nat. M. Sadakane
Department of Applied Chemistry, Graduate School of Advanced
Science and Engineering, Hiroshima University
1-4-1 Kagamiyama, Higashi-Hiroshima 739-8527, Japan
E-mail: sadakane09@hiroshima-u.ac.jp

Supporting information for this article is given via a link at the end of the document.

ARTICLE

mixture diluted in potassium phosphate buffer (pH 8) (Figure 2) showed new redox couples different from the parent $[(\gamma\text{-SiW}_{10}\text{O}_{36})_2\{\text{Ru(IV)(H}_2\text{O)}_4\text{O}_4(\text{OH})_2\}]^{10-}$, indicating the presence of new Ru-containing polyoxometalates. The solvent was removed by evaporation, and the obtained solid was washed with acetone to remove excess pyridine; the obtained black solid was recrystallized by slow diffusion of dimethylformamide to the aqueous solution to form crystals.

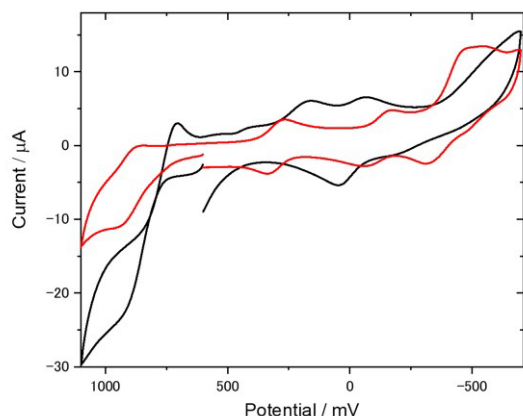


Figure 2. Cyclic voltammograms of the reaction mixture, $[(\gamma\text{-SiW}_{10}\text{O}_{36})_2\{\text{Ru(IV)(H}_2\text{O)}_4\text{O}_4(\text{OH})_2\}]^{10-}$ and pyridine in water, dissolved in phosphate buffer (pH = 8, 0.5 M KH_2PO_4 + 0.5 M KOH). (black) Before heating. (red) The reaction mixture was heated at 80 °C for 3 h. The concentration of the complex was approximately 0.7 mM.

Single-crystal structure analysis revealed that there were two $[(\gamma\text{-SiW}_{10}\text{O}_{36})_2\{\text{Ru(IV)(pyridine)}_4\text{O}_4(\text{OH})_2\}]^{10-}$ molecules in one unit cell where pyridine molecules were coordinated to all the Ru (Figure 1 (c)–(e)). BVS calculations indicate that the oxidation states of Ru and W are 4+ and 6+, respectively, and two bridging oxygens between two Ru atoms are protonated (Table S1), which is similar to $[(\gamma\text{-SiW}_{10}\text{O}_{36})_2\{\text{Ru(IV)(H}_2\text{O)}_4\text{O}_4(\text{OH})_2\}]^{10-}$.^[5, 6] The IR bands of the new compound were similar to those of $[(\gamma\text{-SiW}_{10}\text{O}_{36})_2\{\text{Ru(IV)(H}_2\text{O)}_4\text{O}_4(\text{OH})_2\}]^{10-}$ in the range of 1050–600 cm^{-1} , indicating the presence of the $[(\gamma\text{-SiW}_{10}\text{O}_{36})_2\{\text{Ru(IV)}_4\text{O}_4(\text{OH})_2\}]^{10-}$ structure (Figure 3). Furthermore, the new compound showed characteristic bands at 1484, 1450, and 1213 cm^{-1} assignable to pyridine coordinated to Ru, which is similar to the IR of $[\text{SiW}_{11}\text{O}_{39}\text{Ru(III)(pyridine)}]^{5-}$, where one pyridine coordinates to Ru via Ru–N bond.^[17] Elemental analysis of the novel compound indicated that the ratio of W:Si:Ru:Cs:K was 20:2:4:9:1. These results confirm that the formula for the new compound is $\text{Cs}_9\text{K}[(\gamma\text{-SiW}_{10}\text{O}_{36})_2\{\text{Ru(IV)(pyridine)}_4\text{O}_4(\text{OH})_2\}]$ and the oxidation state of Ru is 4+.

High-resolution electrospray ionization mass spectroscopy (HR-ESI-MS) of the $\text{Cs}_9\text{K}[(\gamma\text{-SiW}_{10}\text{O}_{36})_2\{\text{Ru(IV)(pyridine)}_4\text{O}_4(\text{OH})_2\}]$ dissolved in $\text{H}_2\text{O}-\text{CH}_3\text{CN}$ solution showed a profile assignable to $[\text{H}_4(\gamma\text{-SiW}_{10}\text{O}_{36})_2\{\text{Ru(IV, IV, IV, V)(pyridine)}_4\text{O}_4(\text{OH})_2\}]^{5-}$ (Figure 4), indicating that $[(\gamma\text{-SiW}_{10}\text{O}_{36})_2\{\text{Ru(IV)(pyridine)}_4\text{O}_4(\text{OH})_2\}]^{10-}$ was stable in solution. Oxidation of one Ru was observed, which might have occurred during the electrospray process.

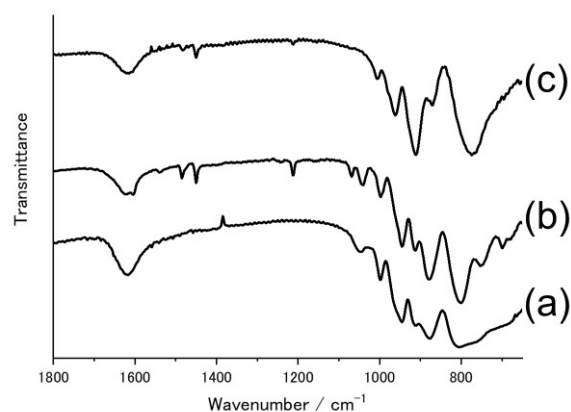


Figure 3. IR spectra of (a) a cesium–potassium mixed salt of $[(\gamma\text{-SiW}_{10}\text{O}_{36})_2\{\text{Ru(IV)(H}_2\text{O)}_4\text{O}_4(\text{OH})_2\}]^{10-}$, (b) cesium–potassium mixed salt of $[(\gamma\text{-SiW}_{10}\text{O}_{36})_2\{\text{Ru(IV)(pyridine)}_4\text{O}_4(\text{OH})_2\}]^{10-}$, and (c) cesium salt of $[\text{SiW}_{11}\text{O}_{39}\text{Ru(III)(pyridine)}]^{5-}$.

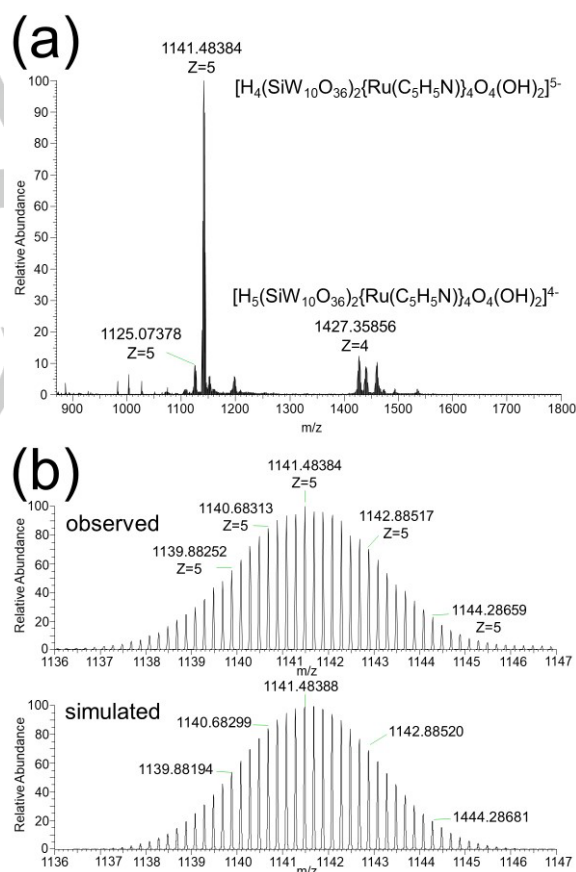


Figure 4. (a) Negative HR-ESI mass spectroscopy of $[(\gamma\text{-SiW}_{10}\text{O}_{36})_2\{\text{Ru(IV)(pyridine)}_4\text{O}_4(\text{OH})_2\}]^{10-}$. (b) Expanded region and simulated profiles for $[\text{H}_4(\gamma\text{-SiW}_{10}\text{O}_{36})_2\{\text{Ru(IV, IV, IV, V)(pyridine)}_4\text{O}_4(\text{OH})_2\}]^{5-}$.

The ^1H NMR spectrum of $[(\gamma\text{-SiW}_{10}\text{O}_{36})_2\{\text{Ru(IV)(pyridine)}_4\text{O}_4(\text{OH})_2\}]^{10-}$ after recrystallization

showed three peaks at 7.22 (doublet), 7.74 (triplet), and 8.43 (triplet) ppm with an intensity ratio of 2:1:2 (Figure 5 (d)) which were assignable to coordinating pyridine because the chemical shifts were different from signals (7.30 (doublet), 7.72 (triplet), and 8.36 (doublet) ppm) of pyridine (Figure 5a). A singlet at 7.78 ppm was assignable to formamide proton of DMF which was used for recrystallization (Figure 5 (d)). The ^1H NMR spectrum of $[(\gamma\text{-SiW}_{10}\text{O}_{36})_2\{\text{Ru}(\text{IV})(\text{pyridine})_4\text{O}_4(\text{OH})_2\}]^{10-}$ before recrystallization showed three peaks at 7.21 (doublet), 7.72 (triplet), and 8.41 (triplet) ppm with an integration ratio of 2:1:2 assignable to the coordinating pyridine (Figure 5 (b)) together with small peaks of unreacted pyridine. Addition of a small amount of pyridine to $[(\gamma\text{-SiW}_{10}\text{O}_{36})_2\{\text{Ru}(\text{IV})(\text{pyridine})_4\text{O}_4(\text{OH})_2\}]^{10-}$ increased the peak intensities of the small peaks (Figure 5 (c)) confirming that unreacted pyridine could not be completely removed by acetone washing. We believe that the three peaks at 7.21 (doublet), 7.72 (triplet), and 8.41 (triplet) ppm are assignable to tetra-pyridine-coordinated species, $[(\gamma\text{-SiW}_{10}\text{O}_{36})_2\{\text{Ru}(\text{IV})(\text{pyridine})_4\text{O}_4(\text{OH})_2\}]^{10-}$, and partially coordinated species such as mono-pyridine coordinated ($[(\gamma\text{-SiW}_{10}\text{O}_{36})_2\{\text{Ru}(\text{IV})(\text{pyridine})_1\{\text{Ru}(\text{IV})(\text{H}_2\text{O})_3\text{O}_4(\text{OH})_2\}]^{10-}$), di-pyridine coordinated ($[(\gamma\text{-SiW}_{10}\text{O}_{36})_2\{\text{Ru}(\text{IV})(\text{pyridine})_2\{\text{Ru}(\text{IV})(\text{H}_2\text{O})_2\text{O}_4(\text{OH})_2\}]^{10-}$), and/or tri-pyridine coordinated ($[(\gamma\text{-SiW}_{10}\text{O}_{36})_2\{\text{Ru}(\text{IV})(\text{pyridine})_3\{\text{Ru}(\text{IV})(\text{H}_2\text{O})_1\text{O}_4(\text{OH})_2\}]^{10-}$) species were not present in D_2O . Reaction mixtures containing small amounts of pyridine, such as when the pyridine/ $[(\gamma\text{-SiW}_{10}\text{O}_{36})_2\{\text{Ru}(\text{IV})(\text{pyridine})_4\text{O}_4(\text{OH})_2\}]^{10-}$ ratio was 1.2 or 2.4, which might contain mono-pyridine, di-pyridine, tri-pyridine, and/or tetra-pyridine-coordinated species, showed different ^1H NMR signals (Figure S1).

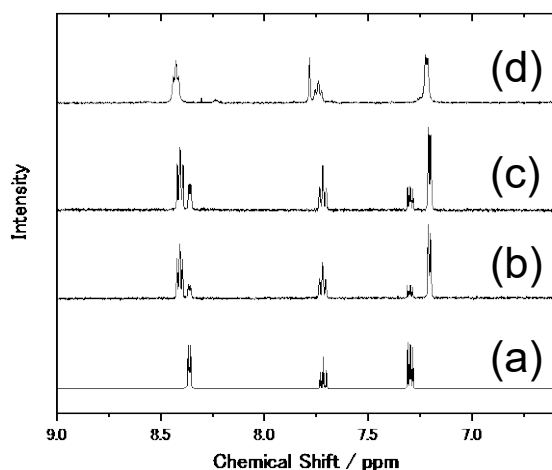
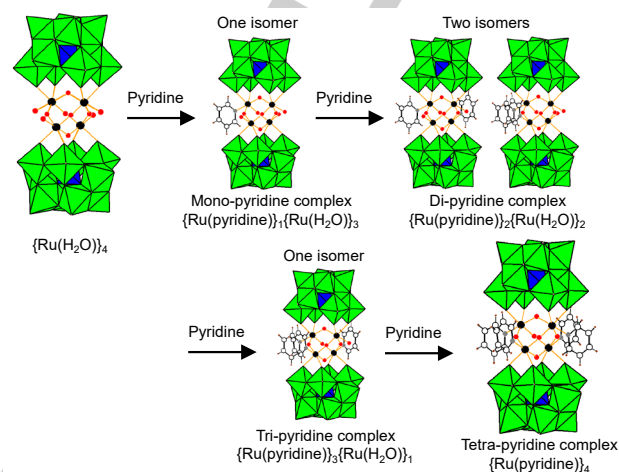


Figure 5. ^1H NMR signals of (a) pyridine, (b) $[(\gamma\text{-SiW}_{10}\text{O}_{36})_2\{\text{Ru}(\text{IV})(\text{pyridine})_4\text{O}_4(\text{OH})_2\}]^{10-}$ before recrystallization, and (c) $[(\gamma\text{-SiW}_{10}\text{O}_{36})_2\{\text{Ru}(\text{IV})(\text{pyridine})_4\text{O}_4(\text{OH})_2\}]^{10-}$ before recrystallization with approximately 1 equivalent of additional pyridine, and (d) $[(\gamma\text{-SiW}_{10}\text{O}_{36})_2\{\text{Ru}(\text{IV})(\text{pyridine})_4\text{O}_4(\text{OH})_2\}]^{10-}$ after recrystallization. Approximately 1.0 mg of the sample was dissolved in 1.0 mL of D_2O .

These results indicate that pyridine coordinates stepwise to the Ru in water to form up to tetra-pyridine coordinated species (Scheme 1), and the once produced tetra-pyridine species is stable in water. Isolation of the partially coordinated species is now underway in our group.



Scheme 1. Stepwise reaction of pyridine to Ru to form tetra-pyridine coordinated species.

Multielectron redox properties. The cyclic voltammogram of $[(\gamma\text{-SiW}_{10}\text{O}_{36})_2\{\text{Ru}(\text{IV})(\text{pyridine})_4\text{O}_4(\text{OH})_2\}]^{10-}$ in an aqueous solution of pH 2 showed six redox couples at 1266 (Py-1), 955 (Py-2), 507 (Py-3), 341 (Py-4), -5 (Py-5), and -394 (Py-6) mV, with a rest potential of approximately 550 mV (Figure 6 (a)). The potential difference between the oxidation and reduction peaks of Py-1 to Py-4 was between 57 mV and 80 mV, indicating that Py-1 to Py-4 is a reversible one-electron transfer process. The cyclic voltammogram of $[(\gamma\text{-SiW}_{10}\text{O}_{36})_2\{\text{Ru}(\text{IV})(\text{H}_2\text{O})_4\text{O}_4(\text{OH})_2\}]^{10-}$ in the same solution showed redox couples (H₂O-1 to H₂O-6) at different potentials (Figure 6(a) and Figure S2), which confirms that $[(\gamma\text{-SiW}_{10}\text{O}_{36})_2\{\text{Ru}(\text{IV})(\text{pyridine})_4\text{O}_4(\text{OH})_2\}]^{10-}$ was stable in the solution, and the pyridine ligand modified the redox potentials of Ru. Furthermore, we observed three ^1H NMR signals in the buffer solution, confirming that $[(\gamma\text{-SiW}_{10}\text{O}_{36})_2\{\text{Ru}(\text{IV})(\text{pyridine})_4\text{O}_4(\text{OH})_2\}]^{10-}$ was stable in the buffer solution (Figure S3).

When the pH of the solution was increased, the redox potentials of Py-1 and Py-2 remained constant, whereas the redox potentials of Py-3 and Py-4 shifted to more negative potentials with slope of 76 and 63 mV/pH, respectively (Figure 6 (b) and (c)). The redox potentials of Py-3 and Py-4 became constant when the pH values of the solution were more than ~5 and ~10, respectively.

The UV-Vis spectroelectrochemical measurements indicated that the redox process Py-3 is one-electron transfer process with redox potential of 321 mV (Figure 7), which agrees well with the redox potential (319 mV) estimated by cyclic voltammetry. These results indicate that the redox couples of Py-1, Py-2, Py-3, and Py-4 correspond to Ru(V, V, IV, IV)/Ru(V, IV, IV, IV), Ru(V, IV, IV, IV)/Ru(IV, IV, IV, IV), Ru(IV, IV, IV, IV)/Ru(IV, IV, IV, III), and Ru(IV, IV, III)/Ru(IV, IV, III, III), respectively. The redox processes of

ARTICLE

Py-1 and Py-2 were not accompanied by protonation/deprotonation, and the redox processes of Py-3 and Py-4 were accompanied by one proton protonation/deprotonation when the pH values of the solution were less than approximately 5 and 10, respectively.^[18]

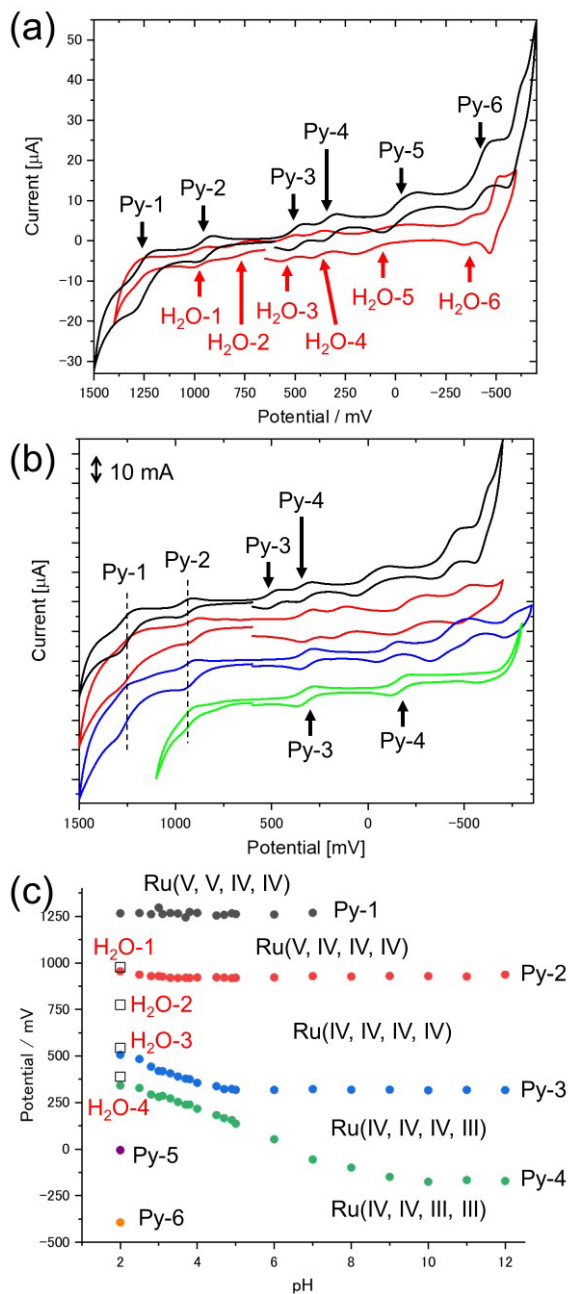


Figure 6. (a) Cyclic voltammograms of (black) $[(\gamma\text{-SiW}_{10}\text{O}_{36})_2\{(\text{Ru}(\text{IV})(\text{pyridine}))_4\text{O}_4(\text{OH})_2\}]^{10-}$ and (red) $[(\gamma\text{-SiW}_{10}\text{O}_{36})_2\{(\text{Ru}(\text{IV})(\text{H}_2\text{O}))_4\text{O}_4(\text{OH})_2\}]^{10-}$ in Britton-Robinson buffer (pH 2.0). (b) Cyclic voltammograms of $[(\gamma\text{-SiW}_{10}\text{O}_{36})_2\{(\text{Ru}(\text{IV})(\text{pyridine}))_4\text{O}_4(\text{OH})_2\}]^{10-}$ in solution with different pH values of (black) 2, (red) 5, (blue) 8, and (green) 12 in Britton-Robinson buffer. (c) Pourbaix diagram of $[(\gamma\text{-SiW}_{10}\text{O}_{36})_2\{(\text{Ru}(\text{IV})(\text{pyridine}))_4\text{O}_4(\text{OH})_2\}]^{10-}$ together with redox potentials (square) of $[(\gamma\text{-SiW}_{10}\text{O}_{36})_2\{(\text{Ru}(\text{IV})(\text{H}_2\text{O}))_4\text{O}_4(\text{OH})_2\}]^{10-}$ (pH 2). Concentration was approximately 0.7 mM.

These results indicate that this new molecule shows a multielectron transfer process over a wide pH range (1–12), which is similar to $[(\gamma\text{-SiW}_{10}\text{O}_{36})_2\{(\text{Ru}(\text{IV})(\text{H}_2\text{O}))_4\text{O}_4(\text{OH})_2\}]^{10-}$.^[19]

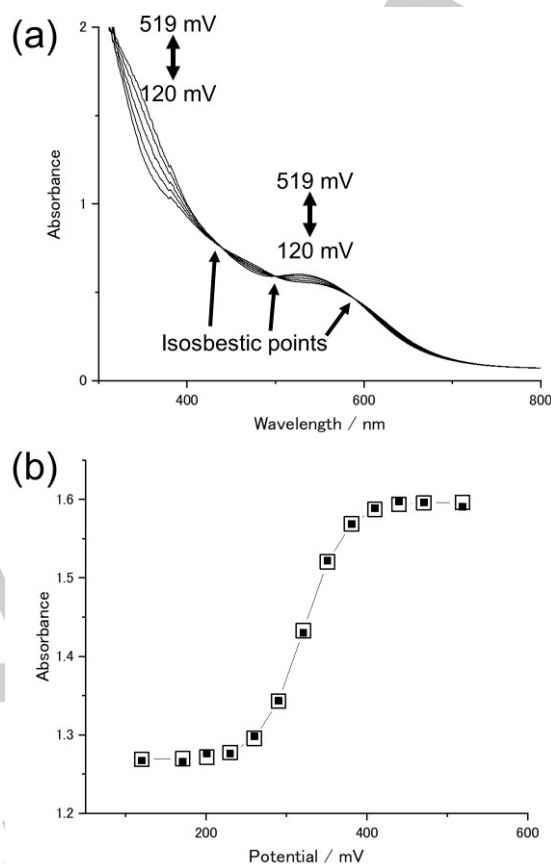


Figure 7. (a) UV-Vis spectra of $[(\gamma\text{-SiW}_{10}\text{O}_{36})_2\{(\text{Ru}(\text{IV})(\text{pyridine}))_4\text{O}_4(\text{OH})_2\}]^{10-}$ (approximately 0.7 mM) dissolved in Britton-Robinson buffer (pH 8.0) with different applied potentials at 519, 351, 321, 290, and 120 mV. (b) Changes in absorbance at 350 nm. Black squares and white squares indicate observed and calculated values, respectively. Calculation was performed using the equation, $A_{\text{obs}} = (A_{\text{red}} + A_{\text{ox}} \times 10^{(E - E_{1/2})/(nF/RT)}) / (1 + 10^{(E - E_{1/2})/(nF/RT)})$, where A_{obs} , A_{red} , A_{ox} , E , $E_{1/2}$, n , F , R , and T represent the observed absorbance, absorbance of the reduced species (1.27), absorbance of the oxidized species (1.60), applied potential, formal potential (321 mV), number of involved electron (1.0), Faraday constant, gas constant, and temperature (298 K), respectively.

Conclusions

Simple mixing of pyridine with $[(\gamma\text{-SiW}_{10}\text{O}_{36})_2\{(\text{Ru}(\text{IV})(\text{H}_2\text{O}))_4\text{O}_4(\text{OH})_2\}]^{10-}$ in water produced a pyridine-coordinated complex that shows a multielectron redox process. The tetra-Ru-oxo core molecule is an active oxidation catalyst, and our results offer a novel modification method for the molecule and redox potentials. Further investigations to produce new materials based on the tetra-Ru-oxo core complex are now underway in our laboratory.

Experimental Section

Homemade deionized water (Millipore, Elix) was used. $K_8[\gamma\text{-SiW}_{10}\text{O}_{36}]\cdot 12\text{H}_2\text{O}$ was prepared according to published literature and were analyzed by IR spectroscopy.^[20, 21] All other chemicals were reagent-grade and used as supplied. Britton–Robinson buffer was prepared by adding NaOH (0.2 M) to a solution containing $\text{CH}_3\text{CO}_2\text{H}$ (0.04 M), H_3PO_4 (0.04 M), and $\text{B}(\text{OH})_3$ (0.04 M), and then, NaNO_3 solid was dissolved in the pH adjusted solution to achieve a concentration of NaNO_3 at 0.5 M.

Preparation of $\text{Cs}_9\text{K}[(\gamma\text{-SiW}_{10}\text{O}_{36})_2\{\text{Ru}_4(\text{H}_2\text{O})_4\text{O}_4(\text{OH})_2\}]\cdot n\text{H}_2\text{O}$. The Cs and K mixed salt of $[(\text{Ru}_4\text{O}_4(\text{OH})_2(\text{H}_2\text{O})_4)(\gamma\text{-SiW}_{10}\text{O}_{36})_2]$ was prepared according to a published procedure with slight modifications, as shown below and analyzed by IR, CV, and UV–Vis spectroscopy^[5, 22].

A solid sample of RuCl_3 (176 mg, 848 μmol) was added to $K_8[\gamma\text{-SiW}_{10}\text{O}_{36}]\cdot 12\text{H}_2\text{O}$ (1.16 g, 424 μmol) dissolved in 50 mL of H_2O . This solution was heated to 80 °C for 5 h and then cooled down to room temperature. The solution was filtered, and then, CsCl (20 mg, 120 μmol) was added and stirred for 20 min. The formed solid was removed by filtration, and CsCl (20 mg) was added to the filtrate. The formed black solid was collected by filtration and dried at 70 °C to form the desired solid (402 mg, 11 % based on W). IR (KBr pellet, cm^{-1}): 999 (m), 947 (m s), 914 (s), 874 (s), 802 (vs), 765 (vs). UV–Vis: $\log \epsilon = 4.65$ at 455 nm (Figure S4) (reported value: $\log \epsilon = 4.57$ at 443 nm)^[5], CV: 1014, 825 (electrochemically irreversible redox), 588, 434, mV (Figure S2) (reported value: 1028, 860, 596, 440)^[22] in 0.1 M HCl.

Preparation of $\text{Cs}_9\text{K}[(\gamma\text{-SiW}_{10}\text{O}_{36})_2\{\text{Ru}_4(\text{C}_5\text{H}_5\text{N})_4\text{O}_4(\text{OH})_2\}]\cdot 3(\text{CH}_3)_2\text{NCHO}\cdot 39\text{H}_2\text{O}$. Cesium–potassium mixed salt of $[(\text{Ru}_4\text{O}_4(\text{OH})_2(\text{H}_2\text{O})_4)(\gamma\text{-SiW}_{10}\text{O}_{36})_2]$ ¹⁰⁻ (120 mg, approximately 16.8 μmol) and 136.4 μl (1.68 mmol) of pyridine were added to 6 mL of H_2O and stirred at 80 °C for 3 h. Then, acetone (120 ml) was added to the solution, and the mixture was dried at 80 °C. After drying, 30 mL acetone was added to the dried solid, and the mixture was ultrasonicated for 5 minutes. The solid was then filtered and the obtained solid was stirred in 5 mL of acetone for 3 min followed by filtration. The washing with acetone and filtration was repeated four times. The solid was dried at 70 °C; the yield was 86 mg and 67% (W-based). Single crystals were obtained by the slow diffusion of DMF into an aqueous solution of compound: Compound (approximately 0.01 g) was dissolved in water (3.0 mL). The vessel containing the solution was placed in a closed beaker containing DMF at room temperature. Elemental analysis for $\text{Cs}_9\text{K}[(\gamma\text{-SiW}_{10}\text{O}_{36})_2\{\text{Ru}_4(\text{C}_5\text{H}_5\text{N})_4\text{O}_4(\text{OH})_2\}]\cdot 3(\text{CH}_3)_2\text{NCHO}\cdot 39\text{H}_2\text{O}$ (7821.69); W 47.3 (calc. 47.0); Si 0.81 (0.79); Ru 4.88 (5.17); Cs 15.3 (15.3); K 0.36 (0.50); C 3.98 (3.99); H 1.28 (1.30); N 1.28 (1.30); Cl < 0.1. ¹H NMR (D_2O): (δ/ppm) 2.71 and 2.86 (s, $(\text{CH}_3)_2\text{NCHO}$), 7.22 (d, 5.1 Hz, 2H, NCH), 7.74 (t, 5.3 Hz, 1H, NCHCH), 7.78 (s, $(\text{CH}_3)_2\text{NCHO}$), 8.43 (t, 3.5 Hz, 2H, NCHCH).

X-Ray crystallography. Single crystals suitable for X-ray diffraction were suspended in mineral oil and mounted on a goniometer head under a nitrogen stream. Intensity data were collected at 123 K on a Bruker SMART equipped with APEX2 CCD detector and Mo $\text{K}\alpha$ microsource ($\lambda = 0.71073$ Å) monochromated by layered confocal mirrors. Data reduction, integration, scaling, and space group determination were carried out using the BRUKER APEX3 suite.^[23] The unit cell was determined by indexing strong reflections, and a tetragonal P lattice was indicated. The data were corrected for absorption effects using numerical methods based on indexed crystal faces.^[23] The initial structure solution by direct methods (SHELXS) located coordinates of heavy atoms, and positions of lighter atoms were revealed through subsequent refinement cycles using the SHELXL program.^[24, 25] The occupancy of cesium and potassium counter cations was refined with SUMP instructions to match the chemical formula

found by total elemental analyses. One oxygen atom (O18) is protonated (bond valence sum = 1.21); its proton is located on the difference map and the O–H distance is fixed at 0.84 Å. Hydrogen atoms on pyridine were placed at the calculated positions. The electron contribution from severely disordered dimethylformamide and some water crystallization solvents was removed from the final model using the PLATON SQUEEZE routine.^[26] All atoms were refined anisotropically. The hydrogen atoms in the crystal waters were not located. The crystallographic data are summarized in Table 1.

Further details of the crystal structure investigation can be obtained from the Cambridge Crystallographic Data Centre (CCDC), 12 Union Road, Cambridge CB2 1EZ, UK [fax.: (internat.) +44 1223/336-033; email: deposit@ccdc.cam.ac.uk], upon quoting the depository numbers CCDC 2131030.

Table 1. Crystal data and structure refinement of $\text{Cs}_9\text{K}[(\text{Ru}_4\text{O}_4(\text{OH})_2(\text{pyridine})_4)(\gamma\text{-SiW}_{10}\text{O}_{36})_2]$.

Chemical formula	$\text{C}_{20}\text{H}_{22}\text{Cs}_9\text{K}_1\text{N}_4\text{O}_{97}\text{Ru}_4\text{Si}_2\text{W}_{20}$
Formula weight, g/mol	7244.51
Temperature (K)	123(2)
Crystal system	Tetragonal
Space group	$P4_2/n$ (#86)
a (Å)	14.0402(7)
c (Å)	33.6966(17)
V (Å ³)	6642.5(7)
Z	2
$D_{\text{calcd.}}$ (g/cm ³)	3.622
μ (mm ⁻¹)	20.252
Radiation	Mo $\text{K}\alpha$ ($\lambda = 0.71073$ Å)
F(000)	6289
Crystal size (mm ³)	0.096 × 0.085 × 0.066
Θ range	1.209 to 27.501°
Index ranges	−18 ≤ h ≤ 18 −18 ≤ k ≤ 18 −43 ≤ l ≤ 43
No. of reflection collected	77409
No. of unique reflections	7631 ($R_{\text{int}} = 0.056$)
Data/restraints/parameters	7631/105/387
G.O.F.	1.087
R indexes [$ I > 2\sigma(I)$]	$R_1^{[a]} = 0.0279$; $wR_2^{[b]} = 0.0562$
R indexes [all data]	$R_1 = 0.0337$; $wR_2 = 0.0579$
$(\Delta/\sigma)_{\text{max}}$	0.001
$(\Delta\rho)_{\text{max/min}}$ (e Å ⁻³)	2.321/−1.129

$$[a] R_1 = \frac{\sum |F_o| - |F_c|}{\sum |F_o|}, [b] wR_2 = \frac{[\sum w(F_o^2 - F_c^2)] / \sum w F_o^2}{1/2} \dots$$

Other analytical techniques

Infrared (IR) spectra were recorded on a NICOLET 6700 FT-IR spectrometer (Thermo Fisher Scientific) using KBr pellets. Cyclic voltammetry was performed on a CHI620D system (BAS Inc.) at ambient temperature. A glassy carbon working electrode (diameter, 3 mm), a platinum wire counter electrode, and an Ag/AgCl reference electrode (203 mV vs. NHE at 25 °C) (3M NaCl, BAS Inc.) were employed. All measurements were performed after N₂ bubbling for 10 min. Approximate formal potential values ($E_{1/2}$ values) were calculated from the cyclic voltammograms as the average of the cathodic and anodic peak potentials for the corresponding oxidation and reduction waves. UV-Vis measurements of electrochemically produced species were performed at ambient temperature using an 8453 UV-Vis spectrophotometer (Agilent) with a 0.5 mm electrochemical quartz cell (SEC-C, BAS Inc.). The working electrode was an Au-mesh electrode. A platinum wire counter electrode and Ag/AgCl reference electrode (203 mV vs. NHE at 25 °C) (3M NaCl, BAS Inc.) were used. The potential was applied using an HAB-151 potentiostat (HOKUTO DENKO Ltd.). ¹H NMR spectra were recorded on a Varian system 500 (500 MHz) spectrometer (Agilent) (H resonance frequency: 499.827 MHz). The spectra were referenced to the internal HOD (4.659 ppm) in D₂O. Elemental analyses were carried out by Mikroanalytisches Labor Pascher (Remagen, Germany). High-resolution ESI-MS spectra were recorded on an LTQ Orbitrap XL (Thermo Fisher Scientific). Five milligrams of each sample was dissolved in 5 mL H₂O by slight heating (stand in an oven heated at 110 °C for 3 minutes), and these solutions were diluted with CH₃CN (final concentration: approximately 10 µg/mL). Peak assignment was performed with accuracy <3 ppm.

Acknowledgements

This research was supported by JSPS KAKENHI (Grant No. JP18H05169 (Grant-in-Aid for Scientific Research on Innovative Areas), International Network on Polyoxometalate Science at Hiroshima University, and the EPSRC-JSPS core-to-core program. Ms. T. Amimoto of the Natural Science Center for Basic Research and Development (N-BARD) at Hiroshima University is acknowledged for performing the ESI-MS measurements. We would like to thank Editage (www.editage.com) for English language editing.

Keywords: Polyoxometalate • Ruthenium • Multielectron Redox

- [1] M. T. Pope, *Heteropoly and Isopoly Oxometalates*, Springer-Verlag, Berlin, 1983.

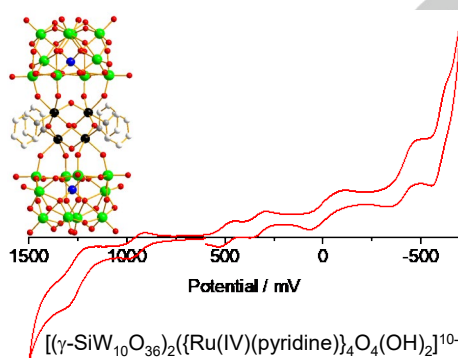
- [2] C. L. Hill, *Chem. Rev.* **1998**, *98*, 1-380.
 [3] L. Cronin, *Chem. Soc. Rev.* **2012**, *41*, 7325-7348.
 [4] S. Yamaguchi, K. Uehara, K. Kamata, K. Yamaguchi, N. Mizuno, *Chem. Lett.* **2008**, *37*, 328-329.
 [5] A. Sartorel, M. Carraro, G. Scorrano, R. D. Zorzi, S. Geremia, N. D. McDaniel, S. Bernhard, M. Bonchio, *J. Am. Chem. Soc.* **2008**, *130*, 5006-5007.
 [6] Y. V. Geletii, B. Botar, P. Kogerler, D. A. Hillesheim, D. G. Musaev, C. L. Hill, *Angew. Chem. Int. Ed.* **2008**, *47*, 3896-3899.
 [7] A. Sartorel, M. Bonchio, S. Campagna, F. Scandola, *Chem. Soc. Rev.* **2013**, *42*, 2262-2280.
 [8] H. Lv, Y. V. Geletii, C. Zhao, J. W. Vickers, G. Zhu, Z. Luo, J. Song, T. Lian, D. G. Musaev, C. L. Hill, *Chem. Soc. Rev.* **2012**, *41*, 7572-7589.
 [9] Y. Liu, S. F. Zhao, S. X. Guo, A. M. Bond, J. Zhang, G. Zhu, C. L. Hill, Y. V. Geletii, *J. Am. Chem. Soc.* **2016**, *138*, 2617-2628.
 [10] M. Bonchio, Z. Syrgiannis, M. Burian, N. Marino, E. Pizzolato, K. Dirian, F. Rigodanza, G. A. Volpato, G. La Ganga, N. Demitri, S. Berardi, H. Amenitsch, D. M. Guldi, S. Caramori, C. A. Bignozzi, A. Sartorel, M. Prato, *Nat. Chem.* **2019**, *11*, 146-153.
 [11] F. M. Toma, A. Sartorel, M. Iurlò, M. Carraro, P. Parisse, C. Maccato, S. Rapino, B. R. Gonzalez, H. Amenitsch, T. Da Ros, L. Casalis, A. Goldoni, M. Marcaccio, G. Scorrano, G. Scoles, F. Paolucci, M. Prato, M. Bonchio, *Nat. Chem.* **2010**, *2*, 826-831.
 [12] M. Sadakane, D. Tsukuma, M. H. Dickman, B. Bassil, U. Kortz, M. Higashijima, W. Ueda, *Dalton Trans.* **2006**, 4271-4276.
 [13] S. Ogo, N. Shimizu, K. Nishiki, N. Yasuda, T. Mizuta, T. Sano, M. Sadakane, *Inorg. Chem.* **2014**, *53*, 3526-3539.
 [14] S. Ogo, N. Shimizu, T. Ozeki, Y. Kobayashi, Y. Ide, T. Sano, M. Sadakane, *Dalton Trans.* **2013**, *42*, 2540-2545.
 [15] M. Sadakane, Y. Imuro, D. Tsukuma, B. S. Bassil, M. H. Dickman, U. Kortz, Y. Zhang, S. Ye, W. Ueda, *Dalton Trans.* **2008**, 6692-6698.
 [16] K. Nishiki, H. Ota, S. Ogo, T. Sano, M. Sadakane, *Eur. J. Inorg. Chem.* **2015**, *2015*, 2714-2723.
 [17] M. Sadakane, S. Moroi, Y. Imuro, N. Izarova, U. Kortz, S. Hayakawa, K. Kato, S. Ogo, Y. Ide, W. Ueda, T. Sano, *Chem. Asian J.* **2012**, *7*, 1331-1339.
 [18] A. J. Bard, L. R. Faulkner, *Electrochemical Methods*, Wiley, New York, **1980**.
 [19] Y. Liu, S. X. Guo, A. M. Bond, J. Zhang, Y. V. Geletii, C. L. Hill, *Inorg. Chem.* **2013**, *52*, 11986-11996.
 [20] A. Tézé, G. Hervé, *Inorg. Synth.* **1990**, *27*, 85-96.
 [21] M. Kikuchi, H. Ota, X. López, T. Nakaya, N. Tsunooji, T. Sano, M. Sadakane, *Eur. J. Inorg. Chem.* **2018**, 1778-1786.
 [22] C. Y. Lee, S. X. Guo, A. F. Murphy, T. McCormac, J. Zhang, A. M. Bond, G. Zhu, C. L. Hill, Y. V. Geletii, *Inorg. Chem.* **2012**, *51*, 11521-11532.
 [23] Bruker, *APEX3, SADABS, SAINT 2016*.
 [24] G. M. Sheldrick, *Acta Crystallogr. C, Struct. Chem.* **2015**, *71*, 3-8.
 [25] C. B. Hubschle, G. M. Sheldrick, B. Dittrich, *J. Appl. Crystallogr.* **2011**, *44*, 1281-1284.
 [26] A. L. Spek, *Acta Crystallogr. C, Struct. Chem.* **2015**, *71*, 9-18.

Entry for the Table of Contents

Layout 1:

FULL PAPER

A pyridine-coordinated tetra-Ru-oxo core sandwich-type silicotungstate, $[(\gamma\text{-SiW}_{10}\text{O}_{36})_2\{\text{Ru(IV)(pyridine)}\}_4\text{O}_4(\text{OH})_2]^{10-}$, was prepared. This molecule showed multielectron redox processes over a wide pH range.



*K. Kokumai, Sugiarto, and M. Sadakane**

Page No. – Page No.

Synthesis and characterization of pyridine-coordinated tetra-Ru-oxo core sandwich-type silicotungstate, $[(\gamma\text{-SiW}_{10}\text{O}_{36})_2\{\text{Ru(IV)(pyridine)}\}_4\text{O}_4(\text{OH})_2]^{10-}$ and its multielectron redox property

Additional Author information for the electronic version of the article.

Author: Kodai Kokumai
Author: Sugiarto
Author: Masahiro Sadakane

ORCID identifier not available
ORCID identifier 0000-0002-4190-2778
ORCID identifier 0000-0001-7308-563X

WILEY-VCH

Supporting Information

Synthesis, characterization, and multielectron redox property of pyridine-coordinated tetra-Ru-oxo core sandwich-type silicotungstate, $[(\gamma\text{-SiW}_{10}\text{O}_{36})_2(\{\text{Ru(IV)(pyridine)}\}_4\text{O}_4(\text{OH})_2)]^{10-}$

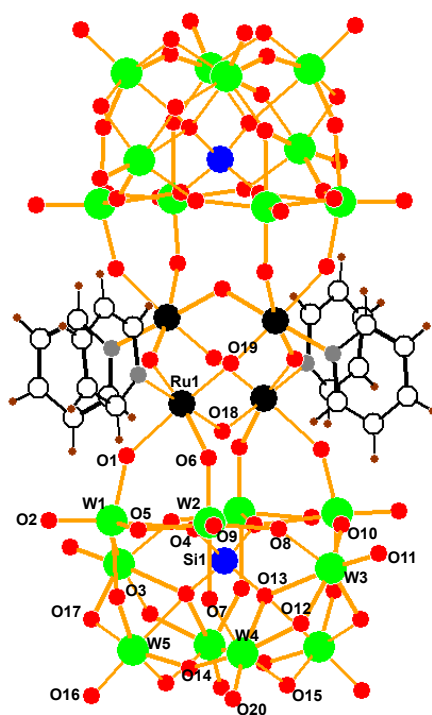
Kodai Kokumai, Sugiarto, Masahiro Sadakane*

Department of Applied Chemistry, Graduate School of Advanced Science and Engineering,
Hiroshima University

1-4-1 Kagamiyama, Higashi-Hiroshima, 739-8527, Japan

Table S1. BVS results obtained using single crystal structure data.

Atom	BVS	Atom	BVS	Atom	BVS
W1	5.82	O3	1.85	O12	1.93
W2	5.87	O4	1.87	O13	1.97
W3	5.99	O5	1.84	O14	1.96
W4	5.91	O6	1.88	O15	1.76
W5	5.94	O7	1.78	O16	1.58
Ru1	4.19	O8	1.99	O17	1.83
Si1	4.01	O9	1.59	O18	1.22
O1	1.90	O10	1.93	O19	1.96
O2	1.62	O11	1.67	O20	1.62



O18 has the lowest BVS amongst the bridging oxygen atoms and was close to 1.0, and is assigned to the OH group.

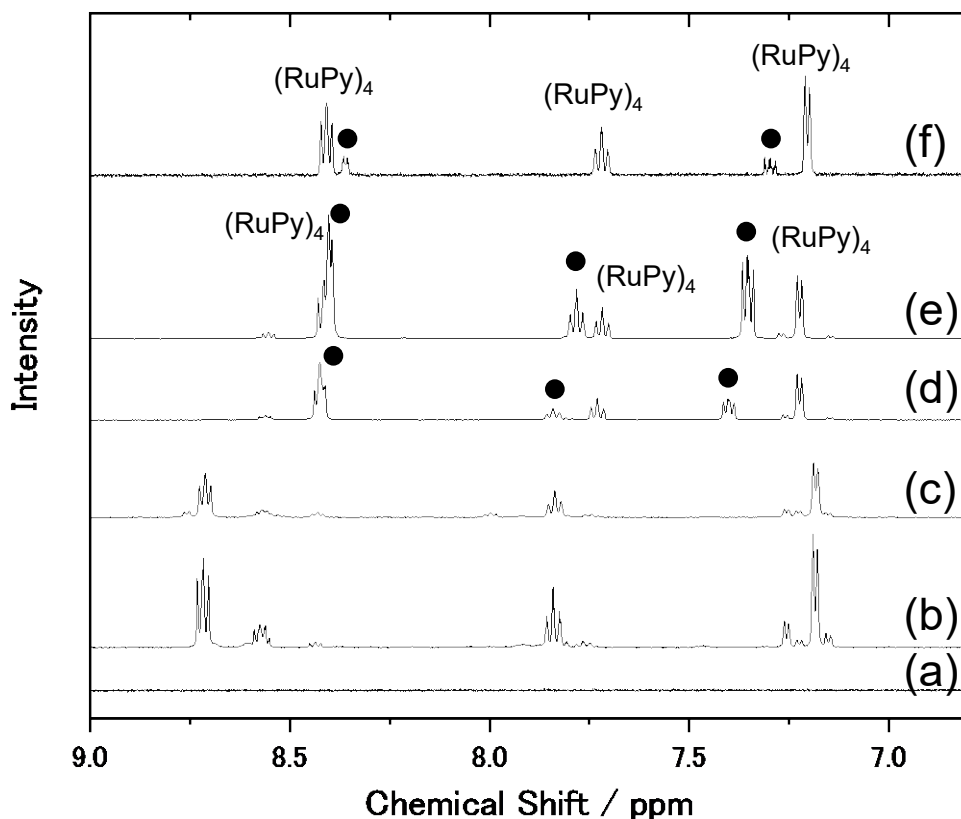


Figure S1. ^1H NMR of (a) $[(\gamma\text{-SiW}_{10}\text{O}_{36})_2(\{\text{Ru(IV)(H}_2\text{O}\})_4\text{O}_4(\text{OH})_2)]^{10-}$ and $[(\gamma\text{-SiW}_{10}\text{O}_{36})_2(\{\text{Ru(IV)(pyridine)}\}_4\text{O}_4(\text{OH})_2)]^{10-}$ with (b) 1.2, (c) 2.4, (d) 7.2 and (e) 12 equivalents of pyridine to $[(\gamma\text{-SiW}_{10}\text{O}_{36})_2(\{\text{Ru(IV)(pyridine)}\}_4\text{O}_4(\text{OH})_2)]^{10-}$ in D_2O . After addition of pyridine, measurements were performed after one hour at room temperature. (f) ^1H NMR of $[(\gamma\text{-SiW}_{10}\text{O}_{36})_2(\{\text{Ru(IV)(pyridine)}\}_4\text{O}_4(\text{OH})_2)]^{10-}$ in D_2O . Black circles indicate peaks corresponding to pyridine, and $(\text{RuPy})_4$ indicate peaks of $[(\gamma\text{-SiW}_{10}\text{O}_{36})_2(\{\text{Ru(IV)(pyridine)}\}_4\text{O}_4(\text{OH})_2)]^{10-}$. Approximately 10 mg of POM samples were dissolved in 1.0 mL D_2O .

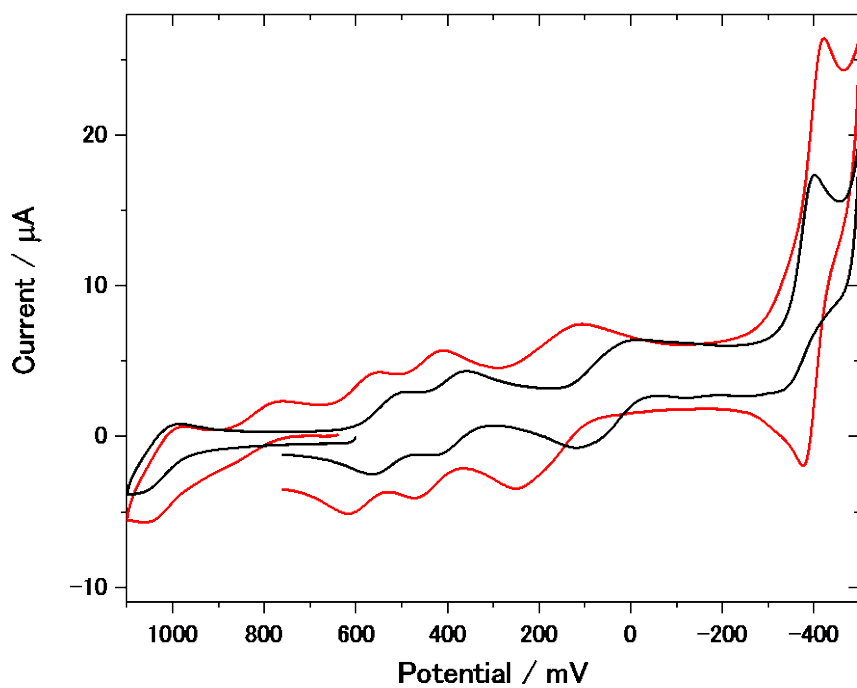


Figure S2. Cyclic voltammograms of (black) $[(\gamma\text{-SiW}_{10}\text{O}_{36})_2(\{\text{Ru(IV)(pyridine)}\}_4\text{O}_4(\text{OH})_2)]^{10-}$ and (red) $[(\gamma\text{-SiW}_{10}\text{O}_{36})_2(\{\text{Ru(IV)(H}_2\text{O)}\}_4\text{O}_4(\text{OH})_2)]^{10-}$ in 0.1 M HCl. Concentration was approximately 0.7 mM.

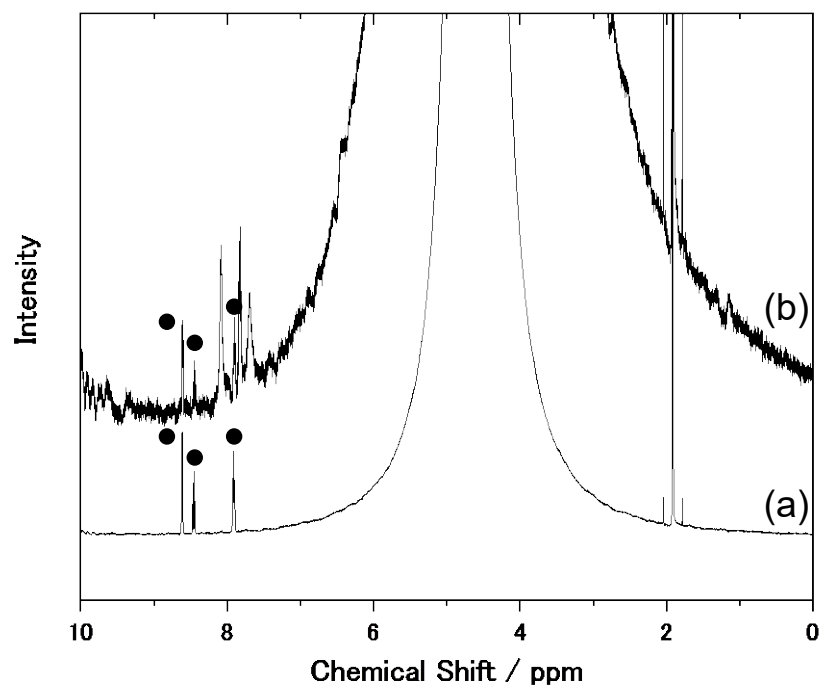


Figure S3. ¹H NMR signals of (a) pyridine and (b) [(γ-SiW₁₀O₃₆)₂({Ru(IV)(pyridine)}₄O₄(OH)₂)]¹⁰⁻ in Britton-Robinson buffer (pH 2.0). Black circles indicate peaks corresponding to pyridine. The peak at approximately 1.95 ppm corresponds to CH₃CO₂H present in the Britton-Robinson buffer, and the large peak at 4.76 ppm corresponds to H₂O.

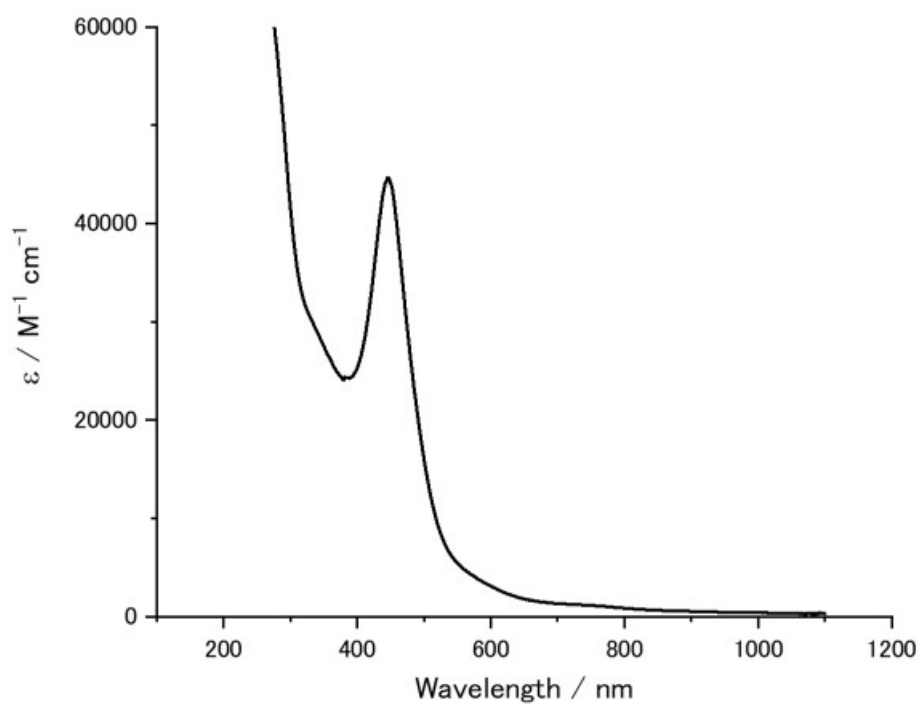


Figure S4. UV-Vis spectra of $[(\gamma\text{-SiW}_{10}\text{O}_{36})_2(\{\text{Ru(IV)(pyridine)}\}_4\text{O}_4(\text{OH})_2)]^{10-}$ in 0.1 M HCl.